Original Article

OPEN

Thermoneutrality induces vascular dysfunction and impaired metabolic function in male Wistar rats: a new model of vascular disease

Amy C. Keller[a,b], Ji H. Chun[c], L.A. Knaub[a,b], M.M. Henckel[a,b], S.E. Hull[a,b], R.L. Scalzo[a,b], G.B. Pott[a,b], L.A. Walker[d], and J.E.B. Reusch[a,b]

Objective: Cardiovascular disease is of paramount importance, yet there are few relevant rat models to investigate its pathology and explore potential therapeutics. Housing at thermoneutral temperature (30 °C) is being employed to humanize metabolic derangements in rodents. We hypothesized that housing rats in thermoneutral conditions would potentiate a high-fat diet, resulting in diabetes and dysmetabolism, and deleteriously impact vascular function, in comparison to traditional room temperature housing (22 °C).

Methods: Male Wistar rats were housed at either room temperature or thermoneutral temperatures for 16 weeks on either a low or high-fat diet. Glucose and insulin tolerance tests were conducted at the beginning and end of the study. At the study's conclusion, vasoreactivity and mitochondrial respiration of aorta and carotid were conducted.

Results: We observed diminished vasodilation in vessels from thermoneutral rats ($P < 0.05$), whereas high-fat diet had no effect. This effect was also observed in endothelium-denuded aorta in thermoneutral rats ($P < 0.05$). Vasoconstriction was significantly elevated in aorta of thermoneutral rats ($P < 0.05$). Diminished nitric oxide synthase activity and nitrotyrosine, and elevated glutathione activity were observed in aorta from rats housed under thermoneutral conditions, indicating a climate of lower nitric oxide and excess reactive oxygen species in aorta. Thermoneutral rat aorta also demonstrated less mitochondrial respiration with lipid substrates compared with the controls ($P < 0.05$).

Conclusion: Our data support that thermoneutrality causes dysfunctional vasoreactivity, decreased lipid mitochondrial metabolism, and modified cellular signaling. These are critical observations as thermoneutrality is becoming prevalent for translational research models. This new model of vascular dysfunction may be useful for dissection of targetable aspects of cardiovascular disease and is a novel and necessary model of disease.

Keywords: cardiovascular disease, , endothelial nitric oxide synthase, mitochondria, thermoneutrality, vasodilation

Abbreviations: ADP, adenosine diphosphate; AMPK, adenosine monophosphate protein kinase; BAT, brown adipose tissue; CVP, cardiovascular disease; cyto c, cytochrome c; eNOS, endothelial nitric oxide synthase; FCCP, carbonyl cyanide-p-trifluoromethoxyphenylhydrazone; G, glutamate; MnSOD, mitochondrial superoxide dismutase; NO, nitric oxide; PGC-1a, peroxisome proliferator-activated receptor gamma coactivator 1-alpha; RCR, respiratory control ratio; ROS, reactive oxygen species; RT, room temperature; S, succinate; SIRT, sirtuin; TBARS, thiobarbituric acid reactive substances; TCA (cycle), tricarboxylic acid cycle, , TNthermoneutrality

INTRODUCTION

Cardiovascular disease (CVD), the leading cause of death in the United States [1], includes all conditions impacting the heart and vasculature, such as hypertension, heart failure, and atherosclerotic cardiovascular disease (ASCVD). CVD risk is significantly elevated in those with diabetes compared with the general population [2], and its progression includes impaired vasoreactivity (dilation and constriction), compromised vascular endothelial function, structural stiffness, increased tone, and vascular mitochondrial dysfunction [3–6]. Vasodilation is regulated by endothelial nitric oxide synthase (eNOS), and this enzyme's activity is compromised in CVD and diabetes [7–11]. We and others have demonstrated that mitochondria are critical to vascular function [12–14] and are

Journal of Hypertension 2022, 40:2133–2146

[a]Division of Endocrinology, Metabolism & Diabetes, University of Colorado Anschutz Medical Campus, [b]Rocky Mountain Regional VA Medical Center, Aurora, Colorado, [c]Microtek, Inc., San Diego, California and [d]Division of Cardiology, University of Colorado Anschutz Medical Campus, Aurora, Colorado, USA

Correspondence to Amy C. Keller, PhD, Assistant Professor/Researcher, Division of Endocrinology, Metabolism & Diabetes, 12801 E. 17th Avenue, 7103, Research 1 South, University of Colorado Anschutz Medical Campus\Rocky Mountain Regional VA Medical Center, 1700 N. Wheeling Street, Aurora, CO 80045, USA.
Tel: +1 303 724 3921; fax: +1 303 724 3920; e-mail: amy.keller@cuanschutz.edu

Received 26 October 2021 **Revised** 3 March 2022 **Accepted** 4 March 2022

DOI:10.1097/HJH.0000000000003153

regulated by eNOS activity in the vasculature [14–16]. Endothelial-mediated vasoreactivity, calcium signaling associated with vascular relaxation, smooth muscle cell proliferation, and apoptosis are processes regulated, in part, by eNOS. Each of these processes require healthy mitochondrial function [17–19]. Vascular mitochondrial dysfunction has been reported in association with smooth muscle cell apoptosis, vascular inflammation, and vascular stiffness [20–22]. In summary, mitochondria are a dominant factor regulating vascular function in myriad ways. Thus, elucidating the connection between mitochondria, eNOS activity, and vascular dysfunction in CVD is critical to a more complete understanding of the pathogenesis of ASCVD.

Animal models demonstrating dysfunction in vascular reactivity and mitochondrial activity within the context of diabetes, metabolic syndrome, or obesity have limitations. Behavioral rat models of diabetes and obesity, such as consuming a high-fat diet, are difficult to calibrate, demonstrate inconsistent vascular structural and functional changes and align poorly with human physiology (such as development of chronic hypertension or development of ASCVD). Rodents can be resistant to the metabolic and cardiovascular impact of cage dwelling (sedentary behavior) and the development of diet-induced obesity and carbohydrate intolerance. As such, most rodent models incompletely and inconsistently recapitulate metabolic disease. Further, many rodent models of ASCVD require genetic changes, such as manipulation of apolipoprotein E or the low-density lipoprotein (LDL) receptor, only available in mice.

Thermoneutrality refers to an environmental temperature where caloric intake is not used to maintain body temperature homeostasis. This temperature is between 14.8 and 24 °C [23] for humans but is 30 °C for rats [24,25]. Animal research environments have traditionally been kept at human thermoneutral temperatures. However, appreciation that this temperature is not thermoneutral for rodents has led to the reevaluation of optimal housing temperatures for rodent research in the modeling of human physiology [26,27]. Thermoneutral housing is now used commonly in rodent metabolic research. Mice and rats housed at thermoneutral conditions show measurable differences in physiology, such as increased energy expenditure rates that align more closely with those of humans, elevated glucose and insulin concentrations, decreased heart rate and blood pressure, and elevated apoptosis proteins [26,28,29]. Thermoneutral housing is reported to increase weight gain and carbohydrate intolerance in rats [26,28,29]. The impact of thermoneutral housing conditions on metabolism and vascular function is somewhat characterized in mice but is unknown in the rat.

We hypothesized that housing rats in thermoneutral conditions would potentiate high-fat diet-induced obesity, resulting in carbohydrate intolerance and impairment in vasoreactivity and mitochondrial function. To test our hypothesis, we housed male rats at either room temperature (RT) or thermoneutrality for 16 weeks and measured metabolic parameters, vasoreactivity, and vascular mitochondrial function. We report here a significant dampening of both vascular function and mitochondrial respiration in aorta, along with metabolic modulation. These effects are present in rats fed either a high-fat or a low-fat diet with little impact of diet on the vascular endpoints. This novel model of thermoneutrality-induced vascular dysfunction is a simple and significant new tool for CVD research and suggests prominent impacts of thermoneutral housing on vascular function.

METHODS AND MATERIALS

Reagents

Western blotting gels were from BioRad (Hercules, California, USA) and PVDF membranes were from Millipore (Burlington, Massachusetts, USA). Collagenase, EDTA, ethylene glycol tetraacetic acid (EGTA), sodium pyrophosphate, sodium orthovanadate, sodium fluoride, okadaic acid, 1% protease inhibitor cocktail, dithiothreitol, magnesium chloride, K-lactobionate, taurine, potassium phosphate, HEPES, digitonin, pyruvate, malic acid, glutamic acid, adenosine diphosphate, succinic acid, oligomycin, carbonyl cyanide 4 (trifluoromethoxy)phenylhydrazone (FCCP), antibody to β-actin (mouse), phenylephrine and acetylcholine, trypsin inhibitor and cytochrome c were procured from Sigma-Aldrich (St Louis, Missouri, USA). Dimethyl sulfoxide (DMSO), sodium chloride, sucrose, and bovine serum albumin were purchased from Fisher Scientific (Pittsburg, Pennsylvania, USA).

Antibodies

Antibodies to total adenosine monophosphate kinase (AMPK, Cell Signaling #2532S, 1 : 500, mouse), phosphorylated AMPK (pAMPK, Cell Signaling #2532S, 1 : 500, rabbit), Sirtuin 1 (SIRT1, Cell Signaling #9475S, 1 : 250, rabbit), Sirtuin 3 (SIRT3, Cell Signaling #2627S, 1 : 500, rabbit), total endothelial nitric oxide synthase (eNOS, Cell Signaling #9572S, 1 : 500, mouse), Ser1177 phosphorylated eNOS (Cell Signaling #9571S, 1 : 500 Rabbit), were obtained from Cell Signaling (Danvers, Massachusetts, USA). Nitrotyrosine was purchased from Cayman Chemical (#10189540, 1 : 500, rabbit, Ann Arbor, Michigan, USA). For the ratio of phosphorylated to total protein, alternate host animal antibodies and alternate secondary antibodies were used with different wavelengths, to eliminate the possibility of signal bleedthrough. Antibody cocktail to representative subunits of mitochondrial oxidative phosphorylation (Total OXPHOS Rodent WB Antibody Cocktail Abcam #ab110413,1 : 1500, mouse) complexes I (subunit NDUF88), II (subunit SDHB), III (subunit UQCRC2), IV (MTCO1), and V (subunit ATP5A), PPARγ coactivator 1 alpha (PGC-1α, Abcam #ab54481, 1 : 500, rabbit) and MnSOD antibody (anti-SOD2/MnSOD antibody [2a1], Abcam, #ab16956, 1 : 500) were obtained from Abcam (Cambridge, Massachusetts, USA). Secondary antibodies were IRDye 800RD goat antimouse #926-68070 at 1 : 10 000, IRDye 800RD goat antirabbit #926-68071 at 1 : 10 000 were purchased from LI-COR (Lincoln, Nebraska, USA) and Starbright Blue 700 goat antimouse at 1 : 5000 #12004159 from Bio-Rad Laboratories.

In-vivo experiments

Animals (male Wistar rats, 5 weeks old), kept at two animals per cage, were housed at either room temperature (22 °C) or thermoneutrality (29–30 °C). Body temperature was taken superficially and elevated temperature was achieved in those housed at thermoneutral conditions as compared

with those house at room temperature (30.4 ± 0.1 vs. 27.4 ± 0.1 °C, $P < 0.001$, data not shown). Animals were fed either a customized diet containing 13% kcal fat (LFD) or 42% kcal fat (HFD) (Envigo [Teklad]) for 16 weeks. Blood (approximately 50 μl) was collected in 0.5 mol/l EDTA and spun at 12 000*g* for 10 min at 4 °C. Plasma was extracted and stored at −80 °C. Fasting blood (6 h) was taken at the beginning and end of the study, fed blood was taken biweekly for glucose and insulin concentrations, and body weight and food consumption were measured weekly. Endpoint parameters were taken at sacrifice, and all animals were euthanized in the morning following ad libitum food consumption.

Vasoreactivity

Sacrifice of animals occurred at 16 weeks, and aortae and carotid vessels were taken from rats at sacrifice, cleaned of fat and tissue, and measured for vasoreactivity using force tension as previously described [30–33]. Denuding was completed mechanically; interior tissue was either rubbed gently with tweezers (aorta) or bubbled with air using a syringe (carotid), and we have previously determined that these techniques result in significantly less response to ACh as compared with intact. We also conducted a Student's *t* test to ensure denuding caused no mechanical damage; we observed no significant differences in paired aorta or carotid. To quantify vasoreactivity, tissue (2 mm rings) was mounted on a stainless steel hook and a force-displacement transducer (Grass Instruments Co., West Warwick, Rhode Island, USA) while incubated in a bath at 1.5 g basal tension for aortae and 1.0 g for carotids; baths contained Krebs buffer (119 mmol/l NaCl, 4.7 mmol/1 KCl, 2.5 mmol/l $CaCl_2$, 1 mmol/l $MgCl_2$, 25 mmol/l $NaHCO_3$, 1.2 mmol/l KH_2PO_4, and 11 mmol/l D-glucose) and continuously bubbled with 95% O_2 and 5% CO_2. Constriction was conducted by exposure to 80 mmol/l KCl. A phenylephrine dose–response curve was also done with doses ranging from 0.002 to 0.7 μmol/l. To investigate vasodilation, a dose–response curve with ACh was performed with a range of 0.05–20 μmol/l secondary to phenylephrine constriction. Data was collected using AcqKnowledge software.

Respiration

Mitochondrial respiration was measured using Oroboros Oxygraph-2k (O2k; Oroboros Instruments Corp., Innsbruck, Austria). The aortae and carotid vessels ($n = 8$) were placed in a mitochondrial preservation buffer [BIOPS (10 mmol/l Ca-EGTA, 0.1 mmol/l free calcium, 20 mmol/l imidazole, 20 mmol/l taurine, 50 mmol/l K-MES, 0.5 mmol/l DTT, 6.56 mmol/l $MgCl_2$, 5.77 mmol/l ATP, 15 mmol/l phosphocreatine, pH 7.1)], stored on ice, cleaned of fat and connective tissue, and permeabilized by incubation with saponin (40 mg/ml) in BIOPS on ice on a shaker for 30 min. The vessels were then washed for 10 min on ice on a shaker in mitochondrial respiration buffer [MiR06 (0.5 mmol/l EGTA, 3 mmol/l magnesium chloride, 60 mmol/l K-lactobionate, 20 mmol/l taurine, 10 mmol/l potassium phosphate, 20 mmol/l HEPES, 110 mmol/l sucrose, 1 g/l bovine serum albumin, 280 U/ml catalase, pH 7.1)]. The vessels were then transferred to MiR06 that had been prewarmed to 37 °C in the chamber of the O2k. Oxygen concentration in the MiR06 started at approximately 400 nmol/ml and was maintained above 250 nmol/ml. Substrates and inhibitors were added to assess respiration rates at several states, including background consumption with carbohydrate or lipid only (state 2), oxidative phosphorylation (+ADP, state 3), maximum oxidative phosphorylation (succinate, state 3S), state 4 (+oligomycin), and uncoupled state (+FCCP). For the carbohydrate experiment, (pyruvate/malate/glutamate-driven), respiration rates were measured with the final concentrations of 5 mmol/l pyruvate + 2 mmol/l malate + 10 mmol/l glutamate, 2 mmol/l adenosine diphosphate (ADP), 6 mmol/l succinate, 4 mg/ml oligomycin, and 0.5 mmol/l stepwise titration of 1 mmol/l carbonyl cyanide 4-trifluoromethoxy) phenylhydrazone (FCCP) until maximal uncoupling (uncoupled state). Only aorta was subjected to the carbohydrate experiment. In the lipid experiment (palmitoylcarnitine-driven respiration), rates were measured with 5 μmol/l palmitoylcarnitine + 1 mmol/l malate, 2 mmol/l ADP, 2 mmol/l glutamate + succinate, 4 mg/ml oligomycin, and 1 mmol/l stepwise titration of FCCP. Cytochrome c (10 mmol/l) was used to determine mitochondrial membrane integrity. Both vessels were subjected to the lipid experiment. Vessels were dried overnight at 60 °C and weighed for dry weight normalization. Using the Oroboros DatLab software, traces were analyzed by averaging a stable trace segment of 3–5 min for each state.

Insulin and glucose intraperitoneal tolerance tests

Insulin tolerance testing (ITT) was done at 1 and 16 weeks of the study, following a 6 h fast, by injection of 1 U/kg body weight of insulin. Blood glucose concentrations were sampled at 0, 15, 30, 45, 60, and 120 min postinjection. Glucose tolerance testing (GTT) followed the same protocol using 1.5 g/kg body weight of glucose, injected intraperitoneally, and was separated from ITT testing by 4 days. Baseline concentrations were subtracted for area under the curve (AUC) analyses. Fasting glucose and insulin concentrations were taken as the 0-min blood collection during GTT.

Western blotting

Aortae were flash-frozen in nitrogen and later processed in mammalian lysis buffer (MPER with 150 mmol/l sodium chloride, 1 mmol/l of EDTA, 1 mmol/l EGTA, 5 mmol/l sodium pyrophosphate, 1 mmol/l sodium orthovanadate, 20 mmol/l sodium fluoride, 500 nmol/l okadaic acid, 1% protease inhibitor cocktail). Aortae were ground under nitrogen with a mortar and pestle, and homogenized at 4 °C and centrifuged first at 1000*g* for 2 min, and supernatants subsequently centrifuged 16 400*g* at 4 °C for 10 min. The Bradford protein assay was used to measure the protein concentration of the lysate. Protein samples (15–40 μg) in Laemmli sample buffer [LSB, boiled with 100 mmol/l dithiothreitol (DTT)] were run on precast SDS-4–15% polyacrylamide gels. Proteins were transferred to PVDF membranes. Quantity One, Bio-Rad, was used to evaluate protein loading. Blots were probed with antibodies described above and left overnight at 4 °C. Fluorescent secondary antibodies were applied following the primary antibody incubation

(1 : 10 000 IRDye800CW, 1 : 10 000 IRDye680RD and Starbright Blue 700), 1 h at room temperature, protected from light). Total and targeted proteins were detected by fluorescence. Total protein was measured using the stain-free gels and associated protocols on the ChemiDoc Imaging System (Bio-Rad, Hercules, California, USA) using the Quantity One 1-D Analysis software (Bio-Rad). All protein data has been normalized to loading control and total protein expression. For determining the ratio of phosphorylated signal to total signal following total protein normalization, antibodies were probed on the same blot using different animal primary antibodies between the phosphorylated and total protein (rabbit vs. mouse) allowing for two color detection and analysis when used with secondary florescent antibodies with differing wavelengths (IRDye 680RD and IRDye 800CW). For nondenatured western blotting, we followed detailed protocols from a previous study [34]. Briefly, samples were prepared with LSB containing 2.5% β-mercaptoethanol, without SDS and DTT, and not denatured. Gels were loaded and run at 4 °C at 20 V overnight in running buffer containing SDS to protect from heat-related denaturing, and transfers were also conducted at 4 °C at 75 V for 2.5 h. eNOS antibody settings, imaging, and analysis were completed as described above.

Glutathione and thiobarbituric acid reactive substances

GSH and thiobarbituric acid reactive substances (TBARS) concentrations were assessed in plasma using kits and instructions from Abcam (Cambridge, UK) and Cayman Chemical (Ann Arbor, Michigan, USA), respectively. For GSH measurements, samples were deproteinated using trichloroacetic acid (TCA) precipitation, according to the kit protocol.

Statistical analysis

To analyze data with time/dose along with diet and temperature, we employed a repeated measures ANOVA, along with a mixed-effects model. For data without a time or dose component, we employed a two-way ANOVA for the variable temperature and diet. Tukey's post hoc analyses were conducted within ANOVA tests. A P value of less than 0.05 was used as the cutoff for statistical significance in all tests. A P value of equal or less than 0.08 was considered indicative of data trends approaching significance.

RESULTS

Metabolic parameters

Rat metabolic parameters were impacted by diet, temperature, or the interaction of these variables across the study (Table 1). Body weights and insulin significantly increased over time ($P < 0.05$ for all), with a high-fat diet resulting in higher weight gain ($P < 0.05$, Table 1); Thermoneutral housing resulted in less weight gain than other groups ($P < 0.05$, Table 1). Fasting insulin concentrations increased to a greater degree in animals housed at thermoneutrality, as well as those on a high-fat diet ($P < 0.05$ for all, Table 1). There was a significant interaction effect of all variables on fasting glucose concentrations ($P < 0.05$, Table 1). AUC of GTT and ITT were higher in those housed at thermoneutrality as compared with diet-matched controls, approaching significance ($P < 0.05$ for all, Table 1). Animals on a high-fat diet had significantly greater gonadal epididymal fat depots than those on a low-fat diet ($P < 0.05$, Table 2). Cardiac fat was unaffected (Table 2).

Housing temperature significantly alters vascular reactivity

To gauge differences in vasoreactivity, aorta and carotid tissue rings were hung on a force transducer and exposed to dose–response curves of vasoconstrictor phenylephrine and vasodilator acetylcholine (ACh). When exposed *ex situ* to vasodilator ACh doses, aorta from rats housed at thermonutrality demonstrated significantly less response as compared with aorta from RT-housed animals ($^{*}P < 0.05$ for dose × temperature interaction, Fig. 1Aa). The compromised vasodilation activity was also seen in carotids from rats housed at thermoneutrality ($^{*}P < 0.05$, Fig. 1Ad). When further analyzed, no effect of diet was noted on aorta or

TABLE 1. Animal weight, fasting glucose and insulin concentrations, and glucose and insulin tolerance test area under the curve at 1 and 16 weeks of treatment

	1 week				16 weeks			
Housing	RT		TN		RT		TN	
diet	LFD	HFD	LFD	HFD	LFD	HFD	LFD	HFD
Weight (g)[a,b,c,d]	199.8 ± 2.6	218.8 ± 3.5	187.5 ± 4.2	182.4 ± 4.3	565.3 ± 12.2	623.3 ± 33.7	516.0 ± 34.1	578.1 ± 24.9
Glucose[e] (mg/dl)	79.8 ± 1.8	86.8 ± 2.2	84.9 ± 3.0	89.1 ± 3.5	70.4 ± 2.6	67.0 ± 2.9	67.2 ± 2.3	72.0 ± 2.4
Insulin[a,b] (μg/ml)	0.5 ± 0.1	0.9 ± 0.2	0.5 ± 0.2	0.7 ± 0.1	1.1 ± 0.2	1.7 ± 0.3	0.9 ± 0.2	1.7 ± 0.4
GTT (AUC)[c]	4031 ± 464	5574 ± 482	4158 ± 523	4693 ± 388	7860 ± 2,361	9599 ± 1271	10 916 ± 1183	12 651 ± 1577
ITT (AUC)	5366 ± 711	4958 ± 454	5214 ± 469	4155 ± 383	4290 ± 509	3754 ± 467	4483 ± 285	4163 ± 330

HFD, high fat diet; LFD, low fat diet; RT, room temperature; TN, thermoneutrality. All parameters had significant effect of time ($P < 0.05$ for all).
[a]$P < 0.05$ diet.
[b]Temperature.
[c]Time × temperature.
[e]Time × diet × temperature effects.
[†]$P < 0.08$ temperature.
[‡]Diet.
[†]Time × temperature, three-way ANOVA, mean ± SEM. GTT AUC reflects integrated glucose concentrations (mg/dl) at time 0, 15, 30, 45, 60, and 120 minutes following an IP glucose injection and ITT AUC is integrated glucose concentrations at the same timepoints following an IP insulin injection. Data were analyzed with mixed-effects and/or repeated measures three-way ANOVA. Data is mean ± SEM.

TABLE 2. Animal cardiac and gonadal–epididymal adipose mass after 16 weeks of treatment

	16 weeks			
Housing	RT		TN	
Diet	LFD	HFD	LFD	HFD
Cardiac fat (g)[†]	0.19 ± 0.02	0.22 ± 0.03	0.28 ± 0.04	0.26 ± 0.02
GE fat (g)[a]	14.78 ± 1.47	22.02 ± 2.55	12.46 ± 1.98	19.49 ± 1.40

HFD, high fat diet; LFD, low fat diet; RT, room temperature; TN, thermoneutrality.
[a]$P < 0.05$ diet.
[b]Temperature
[c]Time × temperature
[d]Time × diet
[e]Time × diet × temperature effects.
[†]$P = 0.05$ temperature effect, two-way ANOVA, mean ± SEM.

carotid (Fig. 1Ab, c, e, f). In endothelium denuded vessels (Fig. 1B), aorta from rats in thermoneutral housing showed less vasodilation than those at RT ($P < 0.05$, temperature effect, Fig. 1Ba). Diet significantly impacted vasodilation in denuded aorta, regardless of housing temperature ($P < 0.05$, diet effect, dose × temperature and diet × temperature interactions, Fig. 1Bb and c). Endothelium denuded carotid from rats housed at thermoneutral condition were significantly less responsive to ACh as compared with those at RT ($P < 0.05$, Fig. 1Bd). Diet did not impact vasodilation in carotids *ex situ* (Fig. 1Be and f). In animals housed at thermoneutrality, phenylephrine response was significantly elevated in aorta as compared with animals housed at RT ($P < 0.05$, Fig. 1C). In aorta, there was a significant effect of both temperature and diet on vasoconstriction ($P < 0.05$ for both, Fig. 1C), not observed in carotids (Fig. 1C).

Thermoneutral housing impacts cellular signaling associated with vasoreactivity and nutrient sensing

To address effects of housing temperature on cellular signaling upstream of vasoreactivity and mitochondrial function, we measured protein expression of nutrient sensor and regulator of eNOS, AMPK, as well as vasodilator eNOS itself. There was a significant interaction effect of diet and temperature on phosphorylated AMPK protein expression in aorta ($P < 0.05$, Fig. 1Da), but no significance was observed in AMPK specific activity (Fig. 1Da). Phosphorylated eNOS was significantly lower in those housed at thermoneutrality ($P < 0.05$, Fig. 11Da). There was a significant interaction effect of temperature × diet, resulting in a greater difference in expression between the room temperature low-fat diet and room temperature high-fat diet groups than between the thermoneutral groups ($P < 0.05$, Fig. 1D). Total eNOS protein expression was not different between groups (Fig. 1D). eNOS specific activity was lower in rats housed at thermoneutrality (Fig. 1D). A nondenatured gel was used to measure dimer and monomer eNOS concentrations in rat aorta (Fig. 1D) to ascertain the presence of the active dimer form or inactive monomer form of eNOS. Monomer protein expression was significantly reduced in those housed at room temperature and on a low-fat diet, indicative of less NO generation, as well as in both groups housed at thermoneutral ($P < 0.05$, Fig. 1D). There were no differences between groups in dimer expression (Fig. 1D). To ascertain whether nitric oxide contributed to a climate of excess reactive nitrogen species, we measured total nitrotyrosine via protein expression. Significantly less nitrotyrosine was observed in aorta from rats housed at thermoneutral ($P < 0.05$, Fig. 1Di).

Lower lipid substrate mitochondrial respiration and altered protein expression of mitochondrial complexes with thermoneutrality

To determine the impact of thermoneutrality on mitochondrial function, we measured mitochondria oxygen consumption using an Oroboros Oxygraph 2k closed chamber. Vessels were exposed to substrates and inhibitors mimicking carbohydrate and lipid metabolism in various states of oxidative phosphorylation. In both aorta and carotid vessels, mitochondrial states 3S (ATP production), 4 (membrane potential maintenance), and uncoupled (maximal uncoupled from ATP production) respiration were significantly diminished in thermoneutrally housed animals ($P < 0.05$ for all, Fig. 2A and B), regardless of diet. In aorta, thermoneutral resulted in significantly less mitochondrial respiration in state 2 ($P < 0.05$, Table 3) and carotid state 3 was diminished with diet, approaching significance ($P < 0.08$, Table 3). No impact on RCR was observed in either vessel (Table 3). To ascertain impacts of thermoneutral housing on mitochondrial complex protein expression, western blotting was used. Thermoneutral housing along with a high-fat diet elevated complex III expression, approaching significance ($P = 0.08$, Fig. 2Cc) Complex IV was also elevated in aorta from animals housed at thermoneutrality, near significance ($P = 0.08$, Fig. 2Cd).

Thermoneutrality is associated with decreased insulin secretion

As a gauge for glucose metabolism, an IP-GTT was performed an all animals. After 16 weeks, insulin secretion concomitant (AUC) with IP-GTT was less in those housed at thermoneutrality on a high-fat diet as compared with room temperature-housed animals (NS, Fig. 3).

Thermoneutrality modifies oxidative stress

To gauge oxidative stress and cellular response, plasma-reduced GSH and TBARS were measured, as well as aorta protein expression of SIRT1 and SIRT3 and cellular and mitochondrial SOD (Fig. 4a). There was a significant diet effect leading to elevated GSH in animals consuming a

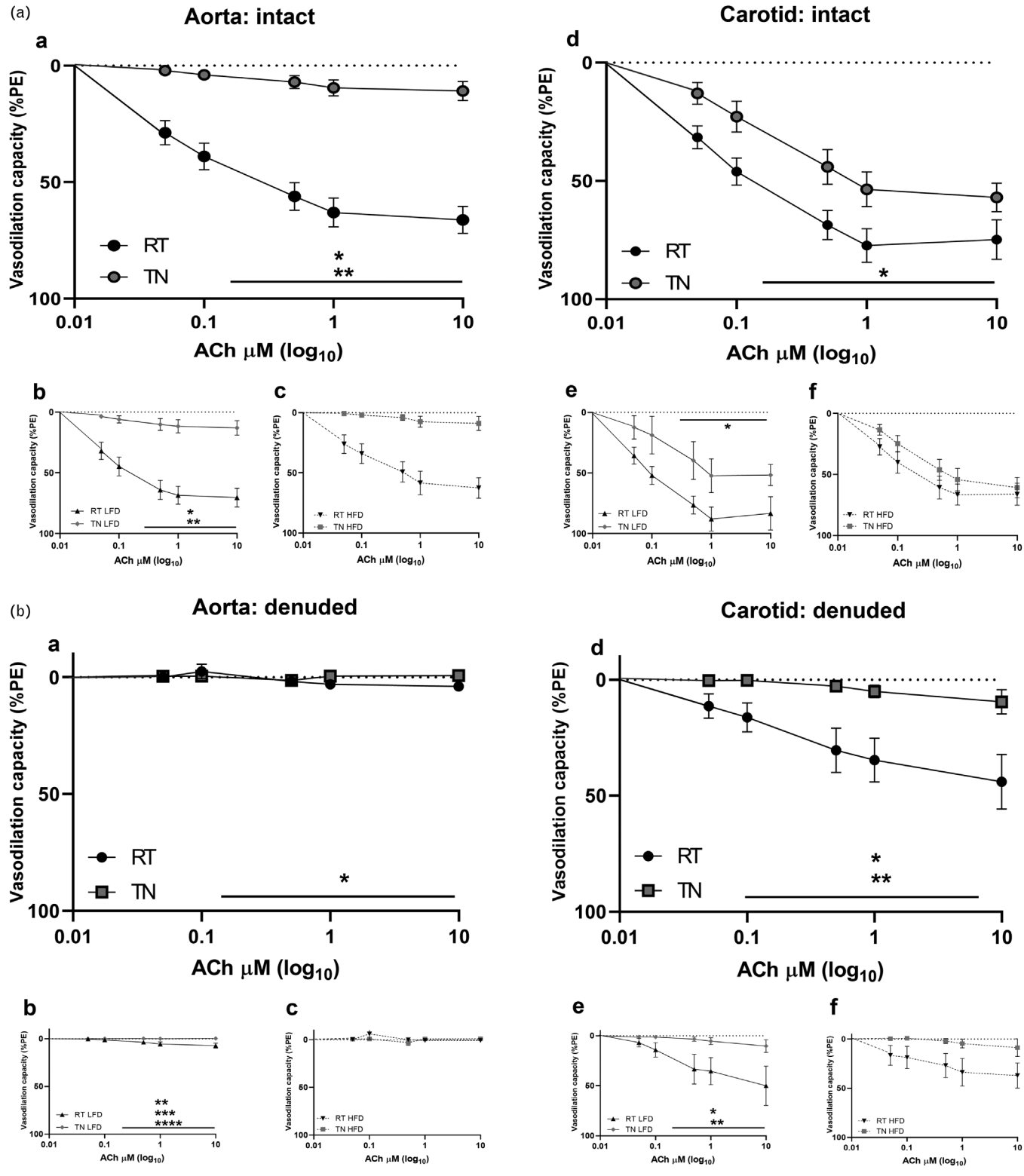

FIGURE 1 (A–D) Vasoreactivity of aorta and carotid intact (A) and denuded (B) in response to acetylcholine or phenylephrine (C), and aorta protein expression of adenosine monophosphate protein kinase and endothelial nitric oxide synthase, western blot experiments (D), dimer and monomer eNOS protein expression, and total nitrotyrosine. Cleaned, intact vessels were attached to a force transducer and exposed to an increased dose of either ACh or PE (A–C). ACh dose–response is expressed as a percentage of fully PE-constricted vessels (A–C). PE dose–response is expressed as mN/mg normalized to vessel wet weight (C). Effect of dose was significant for both ACh and PE ($P < 0.05$). Effects of temperature $^{*}P$ less than 0.05, ACh/PE × temperature interaction ($^{**}P < 0.05$), diet ($^{***}P < 0.05$), diet × temperature interaction ($^{****}P < 0.05$) mixed-effects and/or repeated measures three-way ANOVA (A–C). All vessels are combined according to housing temperature (A, B, and Ca and d) or analyzed together for temperature and diet effect (A and Bb, c, e, f). For D, aorta tissue was processed for protein analysis via western blot analysis, including specific activity (Dc, f, i) ($n = 8$). Blots were probed for pAMPK, AMPK, peNOS, eNOS (Da–i), and nondenatured samples were used for eNOS monomer and dimer detection. Interaction effect (long bar) $^{*}P$ less than 0.05, effect of temperature (elongated bracket), $^{**}P$ less than 0.05, $^{\dagger}P = 0.07$ diet (symbol above data point), two-way ANOVA, (C and D) two-way analysis of variance (ANOVA). Data are mean ± SEM. ACh, acetylcholine; AMPK, adenosine monophosphate protein kinase; eNOS, endothelial nitric oxide synthase; PE, phenylephrine; SEM, standard error of the mean.

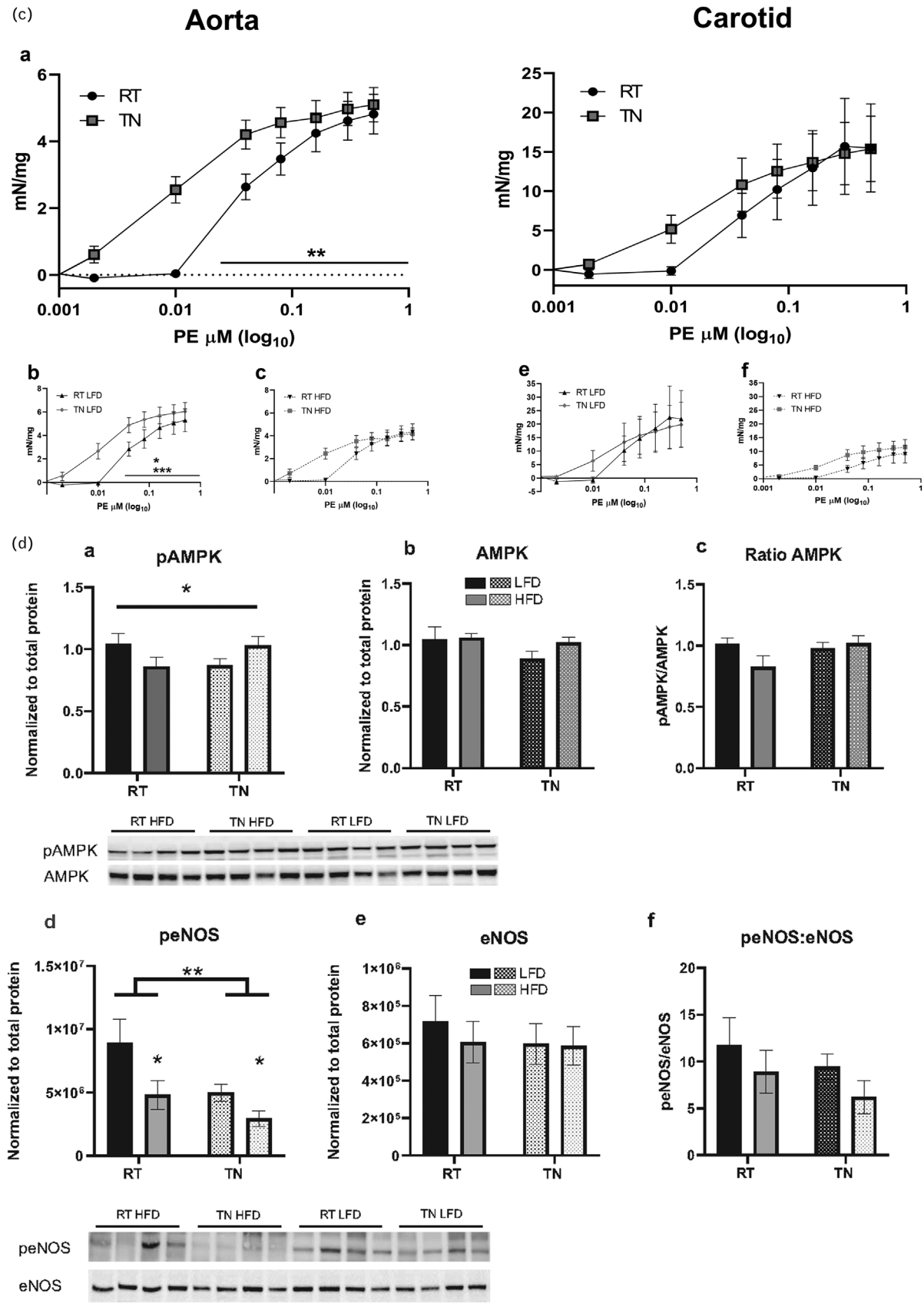

FIGURE 1 Continued

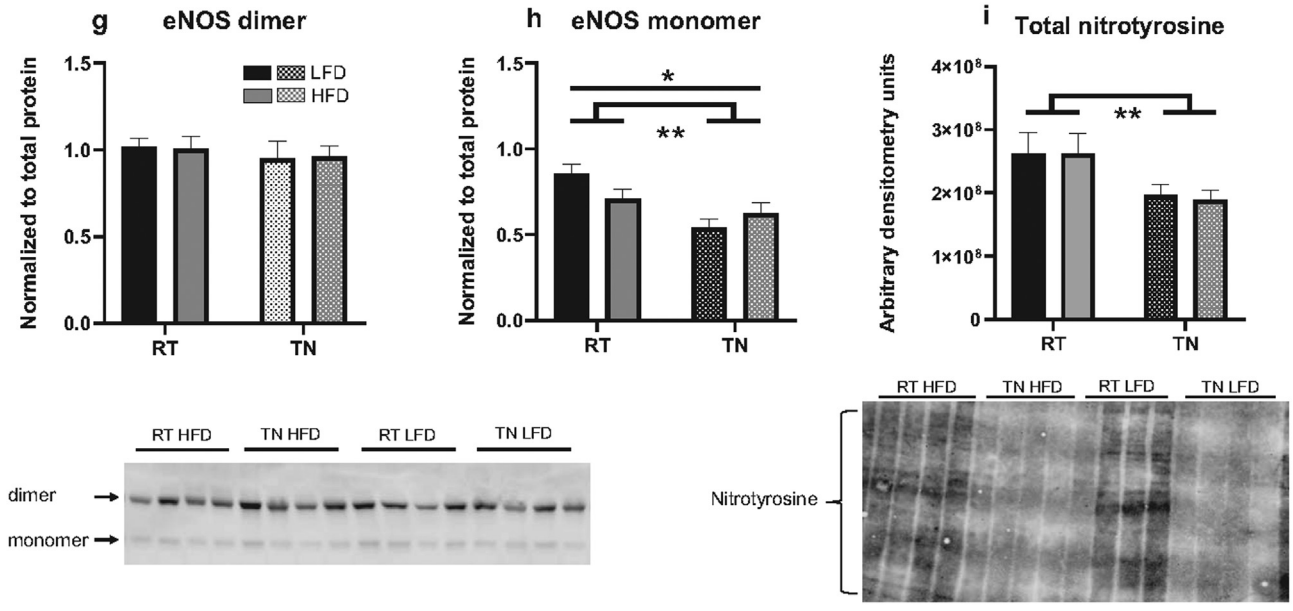

FIGURE 1 Continued

high-fat diet ($P < 0.05$, Fig. 4), with elevated GSH in animals housed at thermoneutrality, approaching significance ($P = 0.06$, Fig. 4). There was a diet effect approaching significance in TBARS concentrations, resulting in elevated concentrations in those on high-fat diets ($P < 0.08$, Fig. 4d), and temperature effect diminishing SIRT1 protein expression ($P < 0.08$, Fig. 4b). There was also a significant interaction effect of temperature and diet on SOD expression ($P < 0.08$, Fig. 4e).

DISCUSSION

Our study tested the impact of thermoneutrality on vasoreactivity and metabolism in the context of low-fat and high-fat diet. We report here that thermoneutrality, in the context of a low-fat diet, led to the impairment of vasodilation and higher constriction in both aorta and carotid. At RT, diet had little-to-no impact on vasoreactivity or mitochondrial function and the impact of thermoneutrality and high-fat diet was not additive. Furthermore, thermoneutral housing lessens insulin secretion with an GTT and did not augment weight gain after 16 weeks. The finding that thermoneutral housing-induced disruption in vascular conduit and resistance artery function, independent of diet, has potential implications for studying human vascular disease. Thermoneutral manipulation generates a novel model of vascular impairment that has the classic clinically relevant functional profiles of endothelial dysfunction, enhanced vasoconstriction, and alterations in vascular mitochondrial function. By utilizing thermoneutral housing, we have characterized a novel driver of vascular disorder and mitochondrial dysfunction, illustrating a new paradigm in which to investigate CVD in both tissue-level functioning and upstream cell signaling.

Rats housed at thermoneutral conditions had a significant impairment in both aorta and carotid ACh-mediated vasodilation consistent with endothelial dysfunction, and thus a prominent role of eNOS. The loss of ACh-mediated vasodilatation in the denuded aorta aligns with endothelial dysfunction. We showed differential response to mechanical denuding in aorta and carotid. This may be because conduit vessels, such as aorta rely more heavily on NO and endothelium-dependent mechanisms for vasodilation than resistance vessels, such as carotid [35]. Our observation that the room temperature carotid responded to ACh could represent incomplete denudation or a difference between the arterial beds. The methods to denude the two vessels are different based on size. Given the similar changes in vasodilatation and vasoconstriction in the intact aorta and carotid, we believe this is a technical problem. Both conduit and resistance vessels from rats housed at thermoneutrality showed a significantly larger response to PE as compared with those from room temperature. Taken together, these functional data are consistent with endothelial dysfunction and eNOS failure. Further, we observed a significant decrease of eNOS activity as evidenced by phosphorylated eNOS protein expression and a lower monomer form of the enzyme in aorta of rats housed at thermoneutrality. This aligns with our observation of total nitrotyrosine, lower in thermoneutral aorta. Diminished eNOS activity and nitrotyrosine in thermoneutrally housed animals suggests a paradigm of ineffective nitric oxide signaling in the vasculature, likely because of NO scavenging in a climate of elevated ROS, agreeing with other studies in humans and rodents [13,14,36–39]. Additionally, our data point to the same mechanism of dysfunction in both conduit (aorta) and resistance (carotid) vessels. This strongly suggests that failed eNOS may be systemic in vasculature of rats housed at thermoneutrality, and thus an informative model of NOS dysregulation.

We demonstrate impaired ACh receptor vasodilation suggesting that NO is not effectively signaling to the smooth muscle. It is possible that nitric oxide is being immediately scavenged or not being produced in favor of eNOS

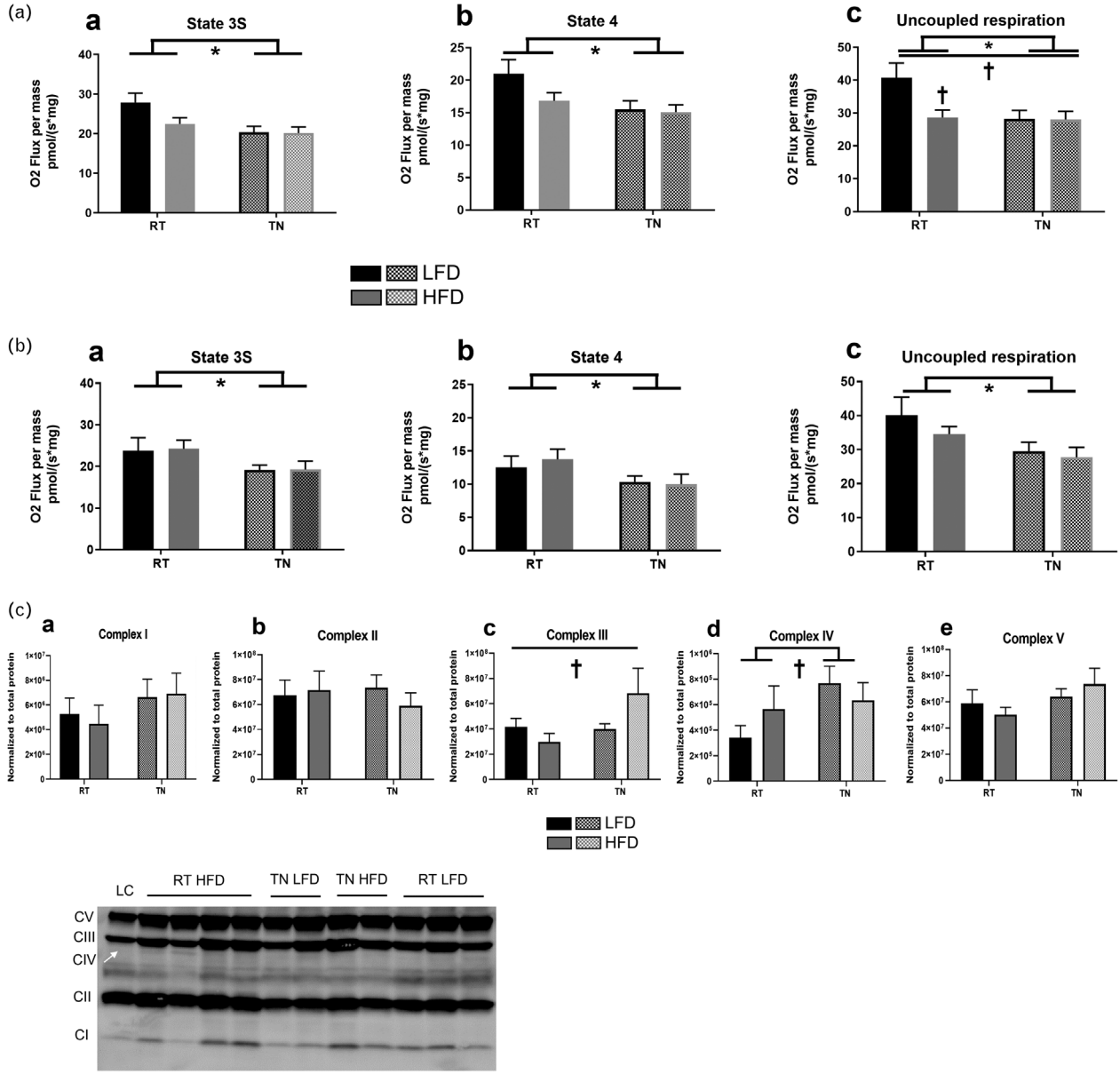

FIGURE 2 (A–C) Mitochondrial respiration in aorta (Aa–c) and carotid (Ba–c), lipid metabolism, and aorta protein expression of mitochondrial complexes (Ca–e). Permeabilized vessels were exposed to substrates and inhibitors mimicking lipid metabolism and background oxygen consumption or leak state (state 2), oxidative phosphorylation (+ADP, state 3), maximum oxidative phosphorylation [succinate, state 3S (A and Ba)], state 4 [+oligomycin (A and Bb), and uncoupled respiration [+FCCP (A and Bc)] were determined. Respiration rates were normalized to tissue dry weight ($n = 7–8$). Effect of temperature $^{*}P$ less than 0.05, ^{+}P less than 0.08, two-way ANOVA. For (Ca–e), aorta tissue was processed for protein analysis via western blot analysis ($n = 8$). Blots were probed for mitochondrial complexes I–IV using a single antibody containing subunits of all complexes. $^{+}P = 0.08$ interaction (long bar) and temperature (elongated bracket) effect, two-way ANOVA; (Ca–e) data are mean ± SEM. ANOVA, analysis of variance.

production of superoxide instead, as known to happen in elevated ROS climates or disrupted eNOS function [40]. This interpretation is supported by the lower levels of nitrotyrosine in thermoneutrally housed rats, despite diminished monomer eNOS activity in these same animals. We observed significantly higher GSH concentrations in plasma from rats housed at thermoneutrality consistent with a climate of elevated ROS; however, TBARS concentrations were not different across groups, indicating that downstream damage from oxidative stress is not significant in this model. Localized excess ROS in the vascular is well known to diminish vasodilation [41,42], likely by scavenging NO, and is also observed in models of chronic disease [43,44], including CVD [7,8,42]. Diminished peNOS expression as well as diminished vasodilation were also observed in aorta of animals housed at RT on a high-fat diet, suggesting that the diminished endothelial and eNOS function we report and also observed in overnutrition, aging, and diabetes [9–11,45–47] may parallel our results from a thermoneutral environment. Taken together, our results support a paradigm of dampened eNOS activity, in turn resulting in diminished local NO production and bioavailability in both conduit and resistance vessels. We cannot rule out that signaling response may be dysfunctional at the

TABLE 3. Mitochondrial respiration states and respiratory control ratios of aorta and carotid

Respiration state/ratio	Aorta RT LFD	Aorta RT HFD	Aorta TN LFD	Aorta TN HFD
2*	4.034 ± 0.79	3.924 ± 0.55	2.612 ± 0.54	2.527 ± 0.45
3	9.211 ± 2.35	6.277 ± 1.09	6.042 ± 1.13	7.392 ± 0.75
RCR	1.351 ± 0.05	1.343 ± 0.05	1.332 ± 0.05	1.336 ± 0.04
Respiration state/ratio	**Carotid RT LFD**	**Carotid RT HFD**	**Carotid TN LFD**	**Carotid TN HFD**
2	4.955 ± 0.80	5.292 ± 0.66	6.065 ± 0.58	4.289 ± 0.92
3†	11.470 ± 1.31	8.395 ± 1.03	9.412 ± 1.26	7.528 ± 1.23
RCR	1.951 ± 0.15	1.816 ± 0.11	1.952 ± 0.21	2.079 ± 0.18

Vessels were exposed to lipid substrates and inhibitors to assess respiration rates at several states, including background oxygen consumption or leak state (state 2), oxidative phosphorylation (+ADP, state 3), maximum oxidative phosphorylation (succinate, state 3S), state 4 (+oligomycin), and uncoupled respiration (+ FCCP). RCR was calculated as state 3S normalized to state 4. HFD, high-fat diet; LFD, low-fat diet; RCR, Respiratory control ratio; RT, room temperature; TN, thermoneutrality.
*P less than 0.05, temperature effect.
†P less than 0.05 diet effect, two-way ANOVA. Data are presented in O_2 flux per mass pmol (s/mg).

level of smooth muscle, such as damaged cGMP or muscle cell performance. Future work will also address the possibility of smooth muscle tissue remodeling and vascular stiffening.

The impact of the thermoneutral environment on vascular mitochondrial function may contribute to abnormal vasomotion. Our results show significantly dampened respiration in aorta and carotid vessels from rats housed at thermoneutrality when exposed to lipid substrates, and elevated mitochondrial complex III and complex V expression. In particular, state 4, a leak state or amount of oxygen consumed with the maintenance of proton gradient and membrane potential, was significantly dampened in aorta from rats housed at thermoneutrality. As damaged membrane potential alters the efficiency of ATP production [48], state 4 may be a driver of the other significantly diminished states in the vessels. Our observations of elevated complex III and IV expression may indicate compensatory activity at the cellular level; our functional data also align directionally with dampened SIRT3 protein expression, a known modulator of mitochondrial function [49,50]. As mitochondrial oxidative phosphorylation processes are coupled to substrates from the TCA cycle, it is intriguing that the diminished respiration observed in thermoneutrally housed rat vessels was only seen when using lipid substrates. This defect in lipid oxidation is suggestive of metabolic flexibility, likely resulting in mitochondrial contributions to a climate of elevated ROS, as previously reported [51–54].

Changes in mitochondrial regulation were observed both at room temperature in response to high-fat diet

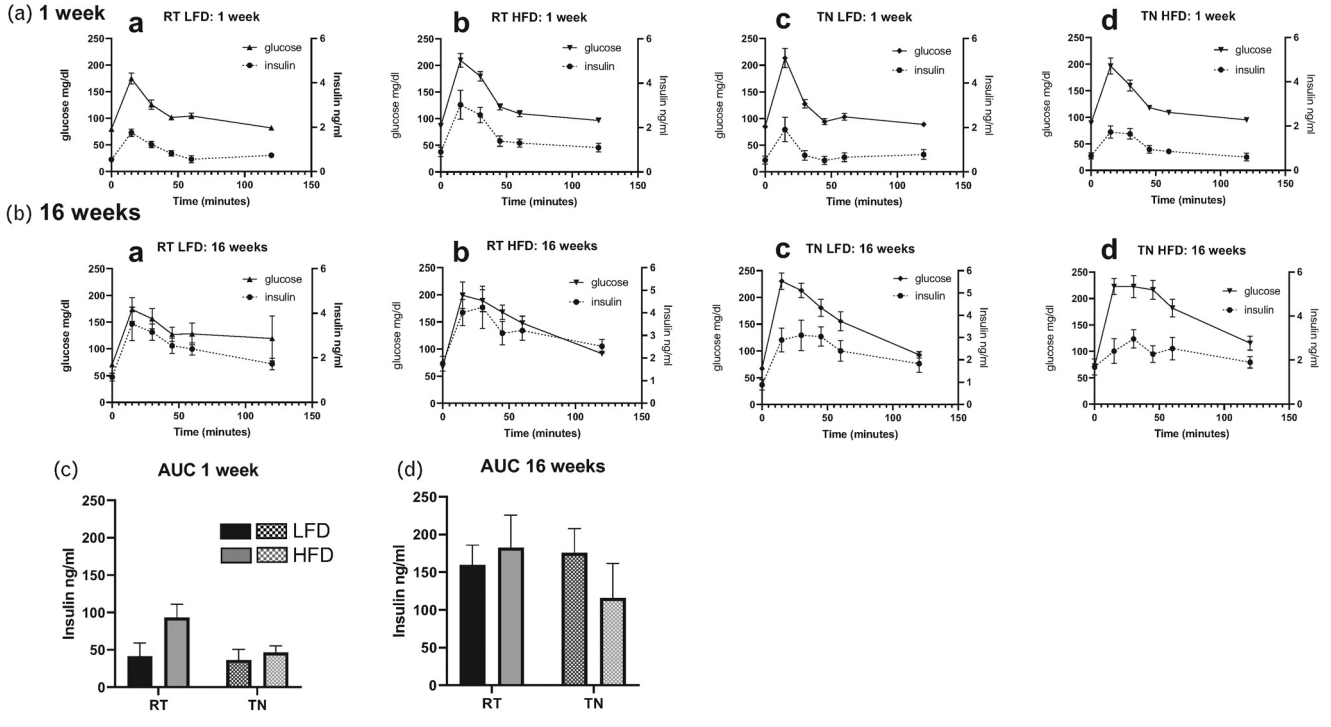

FIGURE 3 (A) Insulin concentrations concurrent with intraperitoneal-glucose tolerance testing. Figures show glucose concentrations (mg/dl) at time 0, 15, 30, 45, 60, and 120 min following an i.p. glucose injection at 1 and 16 weeks of RT LFD (1), thermoneutral LFD (2), RT HFD (3), and thermoneutral HFD (4). Area under the curve (AUC) is represented for each group (5). Effect of time was significant ($P = 0.001$). No other significance was observed, mixed-effects and/or repeated measures three-way ANOVA. Data is mean ± SEM. HFD, high-fat diet; i.p., intraperitoneal; LFD, low-fat diet; RT, room temperature; TN, thermoneutrality.

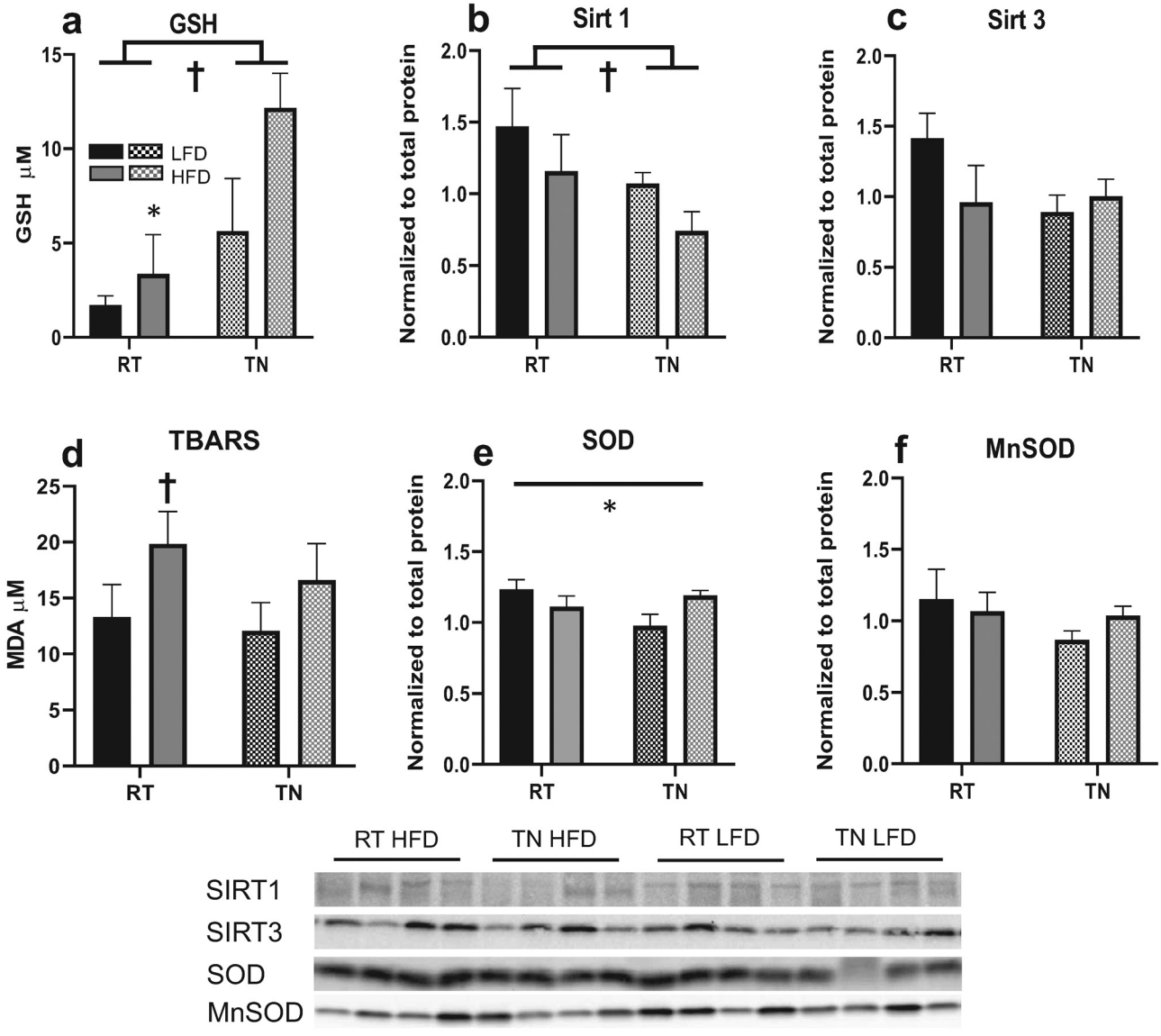

FIGURE 4 Redox profile. In (Aa–d), plasma concentrations of glutathione and thiobarbituric acid reactive substances were assessed ($n = 6–7$). In (Ba–d), aorta tissue was processed for protein analysis via western blot analysis ($n = 8$). Blots were probed for SIRT 1, SIRT3, and MnSOD. Interaction (long bar) effect $^{*}P$ less than 0.05, effect of diet (symbol over data point) $^{**}P$ less than 0.05, $^{***}P$ less than 0.05 temperature (elongated bracket), $^{+}P = 0.05$ temperature, two-way ANOVA. Data are mean ± SEM. ANOVA, analysis of variance; SEM, standard error of the mean.

and at thermoneutrality on both high-fat and low-fat diet. Complex III and V expression are consistent with elevated pAMPK expression observed in rats housed at thermoneutrality. This finding suggests compensatory signaling from AMPK to mitochondrial activation and agrees with previous studies identifying AMPK as an upstream regulator of mitochondria [55,56] in its capacity as a nutrient sensor. These data may reflect that mitochondrial function is suboptimal because of overnutrition or thermoneutral housing; these conditions could decrease or damage bioenergetic demand [57], consistent with our functional respiration data. Conversely, in rats housed at thermoneutrality and fed a high-fat diet, adaptive increases in lipid oxidation would be expected; however, we did not observe this, indicating lower metabolic flexibility, consistent with previous reports [52–55]. Our cellular signaling data in aorta from rats housed at thermoneutrality and fed a high-fat diet underlie a model whereby AMPK is signaling mitochondria to process substrates and generate ATP but this operation is impaired, resulting in increased AMP/ATP ratio and even more AMPK activation further potentiated by overnutrition and/or thermoneutral housing. We and others have shown that NOS regulates mitochondrial function [15,16,58]. In the paradigm we outline here, NOS function upstream of mitochondria may be disrupted by elevated ROS or other factors. This may in turn cause diminished mitochondrial function and ATP production, resulting in altered vascular function because of lack of ATP availability or additional damaging factors cascading from NOS and mitochondrial dysfunction.

After 16 weeks of thermoneutral housing, rats showed a significant dampening of insulin secretion during a glucose tolerance test as compared with room temperature-housed rats. room temperature-housed rats on a low-fat diet

showed a higher insulin secretion resulting in the same glucose concentration area under the curve as those housed at thermoneutrality. We did not observe any differences in glucose handling because of either diet or housing temperature in IP-ITT (data not shown), suggesting that insulin secretion may be impacted, without significant impact on insulin sensitivity.

Our present study contributes to the understanding of thermoneutrality as an emerging method for the generation of animal models aligned with human physiology. Previous studies in mice have shown that thermoneutral housing aligns rodent physiology with that of humans, including similar energy expenditure to basal metabolic rate ratio [26], a cardiovascular profile more similar to that of humans [29], potentiation of high-fat diet-induced diabetes [59,60], and displays general differences in cardiovascular parameters of both rats and mice as compared with room temperature housing [61,62], agreeing with our observed data. Although many studies strongly suggest that thermoneutrality is likely a robust environment for rodent biomedical research and cardiometabolic profiles, the impact of thermoneutrality on the vasculature has not been explored in detail. Very little is known about how thermoneutral housing impacts cellular signaling regulating the vasculature, such as NOS and mitochondria. Here, we contribute to the emerging data on cardiometabolic effects of thermoneutrality by reporting altered vasoreactivity, vascular mitochondrial function, and cellular signaling in aorta and carotid of rats housed at thermoneutrality for 16 weeks. These functional changes make for a novel rat model of vascular dysfunction that recapitulates early endothelial dysfunction observed in human disease (including loss of ACh-mediated vasodilatation and increased response to phenylephrine). These functional phenotypes plus the related changes in NOS and mitochondrial function present a highly clinically relevant mode of vascular disease.

Our study has limitations. We took external body temperature to ascertain whether animals were responding to housing climate; however, this was superficial and not an internal body temperature, and we observed significant physiological differences as a result of different housing temperatures. Housing room temperature was kept at 29–30 °C, which should take into account impacts of co-housing animals on body temperature. It may be possible that at exactly 30 °C, we would observe even more differences. Weight gain was greater in room temperature-housed animals as compared with thermoneutrally housed ones, which differs from reports in mice [59,60]. This could be attributed to the common issue of inconsistent weight gain with overfeeding in rodents in general. Also, we report differential responses in denuded aorta and carotid. Typically, mechanical denuding is different between these vessels and may explain our results. Secondly, aorta is more reliant on endothelial signaling for vasorelaxation that carotid [35], potentially explaining our observations. Also, we use cleaned vessels for our vasoreactivity experiments; they do not contain perivascular adipose tissue (PVAT), adventitia or connective tissue. PVAT acts as a paracrine organ and has considerable regulatory impact on vasodilation and constriction. Although we do not consider PVAT in this study, its impact on the vasculature is a current avenue of investigation in our laboratory. We acknowledge that more studies of rodent physiology comparisons between room temperature and thermoneutral housing are necessary, particularly those that address potential cold stress of housing at room temperature. Thermoneutral housing is an emerging metabolic technique, and additional data will bolster the use of this perturbation in chronic disease studies.

In conclusion, we report a novel rat model of vascular and endothelial dysfunction in response to housing animals at their thermoneutral conditions and independent of diet. The dysfunction of both vasoreactivity in the resistance and conduit vessels and local mitochondrial function aligns with initiating events in human ASCVD pathogenesis. This model also closely aligns with vascular disease profiles observed in human vascular disease, making it a new tool in translational cardiovascular disease in addition to studies of climate on vascular physiology. Our future directions will explore mechanisms connecting these functional observations with an eye on applications to atherosclerosis.

ACKNOWLEDGEMENTS

The authors wish to thank Ms Teri Armstrong and Ms Melissa Blatzer for their kind assistance with the in-vivo measurements, and Mr Jeremy Rahkola and Dr Lori Nield for technical prowess.

Funding sources: the authors wish to acknowledge the following funding sources: NIH/NCRR CCTSI UL1 RR025780, VA Merit (J.E.B.R. BX002046), R01 DK124344-01A1 (J.E.B.R.), VA CDA2 (R.L.S. BX004533 and A.C.K. BX003185), Denver Research Institute, P30DK048520 Colorado Nutrition Obesity Research Center Pilot Award (R.L.S.), and the Ludeman Family Center for Women's Health Research at the University of Colorado Anschutz Medical Campus Junior Faculty Research Development Grants (R.L.S. and A.C.K.), Diabetes Research Center DK116073 (JEBR).

Previous presentations of the data herein:

Chun, J.H., Knaub, L.A., Walker, L.A., Reusch, J.E.-B., Keller, A.C. Delineating sex-specific mechanisms of impaired vasoreactivity in thermoneutrality. April 2021. Department of Medicine Research Day. Aurora, Colorado.

Chun, J.H., Knaub, L.A., Walker, L.A., Reusch, J.E.-B., Keller, A.C. Delineating sex-specific mechanisms of impaired vasoreactivity in thermoneutrality (update). September 2021. American Heart Association Hypertension Scientific Sessions. Virtual.

Author contributions: A.C.K. and J.E.B.R. generated the ideas, wrote the manuscript, housed the project and provided oversight. A.C.K., J.H.C., L.A.K., S.E.H. conducted experiments, generated data, and performed data analysis. M.M.H. and G.B.P. generated data and performed data analysis, and R.L.S. analyzed data. L.A.W. provided experimental oversight and data analysis input.

Data availability statement: the data within this manuscript and that support our reported findings are available from the corresponding author upon reasonable request.

Conflicts of interest

There are no conflicts of interest.

REFERENCES

1. National Institutes of Health National Heart Lung and Blood Institute. Know the Difference Fact Sheet. 2021 [cited 2021 April 14]; Available at: https://www.nhlbi.nih.gov/health-topics/all-publications-and-resources/know-differences-cardiovascular-disease-heart-disease-coronary-heart-diseae [Accessed October 2021].
2. Bloomgarden Z. Cardiovascular disease and diabetes. *Diabetes Care* 2003; 26:230–237.
3. Gibbons GH, Dzau VJ. The emerging concept of vascular remodeling. *Engl J Med* 1994; 19:1431–1438.
4. Kizhakekuttu TJ, Wang J, Dharmashankar K, Ying R, Gutterman DD, Vita JA, Widlansky ME. Adverse alterations in mitochondrial function contribute to type 2 diabetes mellitus-related endothelial dysfunction in humans. *Arterioscler Thromb Vasc Biol* 2012; 32:2531–2539.
5. Laurent S, Alivon M, Beaussier H, Boutouyrie P. Aortic stiffness as a tissue biomarker for predicting future cardiovascular events in asymptomatic hypertensive subjects. *Ann Med* 2012; 44 (Suppl 1):S93–S97.
6. Zieman SJ, Melenovsky V, Kass DA. Mechanisms, pathophysiology, and therapy of arterial stiffness. *Arterioscler Thromb Vasc Biol* 2005; 25:932–943.
7. Deanfield JE, Halcox JP, Rabelink TJ. Endothelial function and dysfunction: testing and clinical relevance. *Circulation* 2007; 115:1285–1295.
8. Endemann DH, Schiffrin EL. Endothelial dysfunction. *J Am Soc Nephrol* 2004; 15:1983–1992.
9. Ding H, Triggle CR. Endothelial cell dysfunction and the vascular complications associated with type 2 diabetes: assessing the health of the endothelium. *Vasc Health Risk Manag* 2005; 1:55–71.
10. McVeigh GE, Brennan GM, Johnston GD, McDermott BJ, McGrath LT, Henry WR, *et al*. Impaired endothelium-dependent and independent vasodilation in patients with type 2 (noninsulin-dependent) diabetes mellitus. *Diabetologia* 1992; 35:771–776.
11. Thum T, Fraccarollo D, Schultheiss M, Froese S, Galuppo P, Widder JD, *et al*. Endothelial nitric oxide synthase uncoupling impairs endothelial progenitor cell mobilization and function in diabetes. *Diabetes* 2007; 56:666–674.
12. Keller AC, Knaub LA, Miller MW, Birdsey N, Klemm DJ, Reusch JE. Saxagliptin restores vascular mitochondrial exercise response in the Goto-Kakizaki rat. *J Cardiovasc Pharmacol* 2015; 65:137–147.
13. Keller AC, Knaub LA, Scalzo RL, Hull SE, Johnston AE, Walker LA, Reusch JEB. Sepiapterin improves vascular reactivity and insulin-stimulated glucose in Wistar rats. *Oxid Med Cell Longev* 2018; 2018:7363485.
14. Miller MW, Knaub LA, Olivera-Fragoso LF, Keller AC, Balasubramaniam V, Watson PA, *et al*. Nitric oxide regulates vascular adaptive mitochondrial dynamics. *Am J Physiol Heart Circ Physiol* 2013; 304: H1624–H1633.
15. Nisoli E, Clementi E, Paolucci C, Cozzi V, Tonello C, Sciorati C, *et al*. Mitochondrial biogenesis in mammals: the role of endogenous nitric oxide. *Science* 2003; 299:896–899.
16. Nisoli E, Tonello C, Cardile A, Cozzi V, Bracale R, Tedesco L, *et al*. Calorie restriction promotes mitochondrial biogenesis by inducing the expression of eNOS. *Science* 2005; 310:314–317.
17. Salabei JK, Hill BG. Mitochondrial fission induced by platelet-derived growth factor regulates vascular smooth muscle cell bioenergetics and cell proliferation. *Redox Biol* 2013; 1:542–551.
18. Sward K, Dreja K, Lindqvist A, Persson E, Hellstrand P. Influence of mitochondrial inhibition on global and local [Ca(2+)](I) in rat tail artery. *Circ Res* 2002; 90:792–799.
19. Taggart MJ, Wray S. Hypoxia and smooth muscle function: key regulatory events during metabolic stress. *J Physiol* 1998; 509 (Pt 2):315–325.
20. Davidson SM. Endothelial mitochondria and heart disease. *Cardiovasc Res* 2010; 88:58–66.
21. Ungvari Z, Sonntag WE, Csiszar A. Mitochondria and aging in the vascular system. *J Mol Med (Berl)* 2010; 88:1021–1027.
22. Zhou B, Tian R. Mitochondrial dysfunction in pathophysiology of heart failure. *J Clin Invest* 2018; 128:3716–3726.
23. Kingma BR, Frijns AJ, Schellen L, van Marken Lichtenbelt WD. Beyond the classic thermoneutral zone: Including thermal comfort. *Temperature (Austin)* 2014; 1:142–149.
24. Romanovsky AA, Ivanov AI, Shimansky YP. Selected contribution: ambient temperature for experiments in rats: a new method for determining the zone of thermal neutrality. *J Appl Physiol (1985)* 2002; 92:2667–2679.
25. Poole S, Stephenson JD. Body temperature regulation and thermoneutrality in rats. *Q J Exp Physiol Cogn Med Sci* 1977; 62:143–149.
26. Fischer AW, Cannon B, Nedergaard J. Optimal housing temperatures for mice to mimic the thermal environment of humans: an experimental study. *Mol Metab* 2018; 7:161–170.
27. Keijer J, Li M, Speakman JR. What is the best housing temperature to translate mouse experiments to humans? *Mol Metab* 2019; 25:168–176.
28. Aldiss P, Symonds ME, Lewis JE, Boocock DJ, Miles AK, Bloor I, *et al*. Interscapular and perivascular brown adipose tissue respond differently to a short-term high-fat diet. *Nutrients* 2019; 11:1065.
29. Overton JM. Phenotyping small animals as models for the human metabolic syndrome: thermoneutrality matters. *Int J Obes (Lond)* 2010; 34 (Suppl 2):S53–S58.
30. Keller AC, Knaub LA, McClatchey PM, Connon CA, Bouchard R, Miller MW, *et al*. Differential mitochondrial adaptation in primary vascular smooth muscle cells from a diabetic rat model. *Oxid Med Cell Longevity* 2016; 2016: 2016:8524267.
31. Babu GJ, Pyne GJ, Zhou Y, Okwuchukuasanya C, Brayden JE, Osol G, *et al*. Isoform switching from SM-B to SM-A myosin results in decreased contractility and altered expression of thin filament regulatory proteins. *Am J Physiol Cell Physiol* 2004; 287:C723–C729.
32. Sutliff RL, Paul RJ. Smooth muscle studies using gene-altered mouse models: a users guide. In: Hoit BD, Walsh RA, editors. *Cardiovascular physiology in the genetically engineered mouse*. Boston: Kluwer; 1998.
33. Walker LA, Gailly P, Jensen PE, Somlyo AV, Somlyo AP. The unimportance of being (protein kinase C) epsilon. *FASEB J* 1998; 12:813–821.
34. Chang F, Flavahan S, Flavahan NA. Potential pitfalls in analyzing structural uncoupling of eNOS: aging is not associated with increased enzyme monomerization. *Am J Physiol Heart Circ Physiol* 2019; 316: H80–H88.
35. Wenceslau CF, McCarthy CG, Earley S, England SK, Filosa JA, Goulopoulou S, *et al*. Guidelines for the measurement of vascular function and structure in isolated arteries and veins. *Am J Physiol Heart Circ Physiol* 2021; 321:H77–H111.
36. Nilsson H, Aalkjaer C. Vasomotion: mechanisms and physiological importance. *Mol Interv* 2003; 3:79–8951.
37. Knaub LA, McCune S, Chicco AJ, Miller M, Moore RL, Birdsey N, *et al*. Impaired response to exercise intervention in the vasculature in metabolic syndrome. *Diab Vasc Dis Res* 2013; 10:222–238.
38. Heitzer T, Schlinzig T, Krohn K, Meinertz T, Munzel T. Endothelial dysfunction, oxidative stress, and risk of cardiovascular events in patients with coronary artery disease. *Circulation* 2001; 104:2673–2678.
39. Jin RC, Loscalzo J. Vascular nitric oxide: formation and function. *J Blood Med* 2010; 2010:147–162.
40. Vasquez-Vivar J, Kalyanaraman B, Martasek P, Hogg N, Masters BS, Karoui H, *et al*. Superoxide generation by endothelial nitric oxide synthase: the influence of cofactors. *Proc Natl Acad Sci U S A* 1998; 95:9220–9225.
41. Kawashima S. The two faces of endothelial nitric oxide synthase in the pathophysiology of atherosclerosis. *Endothelium* 2004; 11:99–107.
42. Forstermann U, Xia N, Li H. Roles of vascular oxidative stress and nitric oxide in the pathogenesis of atherosclerosis. *Circ Res* 2017; 120:713–735.
43. Bashan N, Kovsan J, Kachko I, Ovadia H, Rudich A. Positive and negative regulation of insulin signaling by reactive oxygen and nitrogen species. *Physiol Rev* 2009; 89:27–71.
44. Youn JY, Siu KL, Lob HE, Itani H, Harrison DG, Cai H. Role of vascular oxidative stress in obesity and metabolic syndrome. *Diabetes* 2014; 63:2344–2355.
45. Meziat C, Boulghobra D, Strock E, Battault S, Bornard I, Walther G, Reboul C. Exercise training restores eNOS activation in the perivascular adipose tissue of obese rats: Impact on vascular function. *Nitric Oxide* 2019; 86:63–67.
46. Lee HY, Zeeshan HMA, Kim HR, Chae HJ. Nox4 regulates the eNOS uncoupling process in aging endothelial cells. *Free Radic Biol Med* 2017; 113:26–35.
47. Xia N, Horke S, Habermeier A, Closs EI, Reifenberg G, Gericke A, *et al*. Uncoupling of endothelial nitric oxide synthase in perivascular adipose tissue of diet-induced obese mice. *Arterioscler Thromb Vasc Biol* 2016; 36:78–85.
48. Zorova LD, Popkov VA, Plotnikov EY, Silachev DN, Pevzner IB, Jankauskas SS, *et al*. Mitochondrial membrane potential. *Anal Biochem* 2018; 552:50–59.
49. Ahn BH, Kim HS, Song S, Lee IH, Liu J, Vassilopoulos A, *et al*. A role for the mitochondrial deacetylase Sirt3 in regulating energy homeostasis. *Proc Natl Acad Sci U S A* 2008; 105:14447–14452.

50. Finley LW, Haas W, Desquiret-Dumas V, Wallace DC, Procaccio V, Gygi SP, Haigis MC. Succinate dehydrogenase is a direct target of sirtuin 3 deacetylase activity. *PLoS One* 2011; 6:e23295.
51. Keller A, Hull SE, Elajaili H, Johnston A, Knaub LA, Chun JH, *et al.* (-)-Epicatechin modulates mitochondrial redox in vascular cell models of oxidative stress. *Oxid Med Cell Longev* 2020; 2020:6392629.
52. Nishikawa T, Edelstein D, Du XL, Yamagishi S, Matsumura T, Kaneda Y, *et al.* Normalizing mitochondrial superoxide production blocks three pathways of hyperglycaemic damage. *Nature* 2000; 404:787–790.
53. Rizwan H, Pal S, Sabnam S, Pal A. High glucose augments ROS generation regulates mitochondrial dysfunction and apoptosis via stress signalling cascades in keratinocytes. *Life Sci* 2020; 241:117148.
54. Rosca MG, Vazquez EJ, Chen Q, Kerner J, Kern TS, Hoppel CL. Oxidation of fatty acids is the source of increased mitochondrial reactive oxygen species production in kidney cortical tubules in early diabetes. *Diabetes* 2012; 61:2074–2083.
55. Keller AC, Knaub LA, McClatchey PM, Connon CA, Bouchard R, Miller MW, *et al.* Differential mitochondrial adaptation in primary vascular smooth muscle cells from a diabetic rat model. *Oxid Med Cell Longev* 2016; 2016:8524267.
56. Zhang H, Liu B, Li T, Zhu Y, Luo G, Jiang Y, *et al.* AMPK activation serves a critical role in mitochondria quality control via modulating mitophagy in the heart under chronic hypoxia. *Int J Mol Med* 2018; 41:69–76.
57. Moellering DR, Smith DL Jr. Ambient temperature and obesity. *Curr Obes Rep* 2012; 1:26–34.
58. Chen Z, Peng IC, Cui X, Li YS, Chien S, Shyy JY. Shear stress, SIRT1, and vascular homeostasis. *Proc Natl Acad Sci U S A* 2010; 107:10268–10273.
59. Stemmer K, Kotzbeck P, Zani F, Bauer M, Neff C, Muller TD, *et al.* Thermoneutral housing is a critical factor for immune function and diet-induced obesity in C57BL/6 nude mice. *Int J Obes (Lond)* 2015; 39:791–797.
60. Ganeshan K, Chawla A. Warming the mouse to model human diseases. *Nat Rev Endocrinol* 2017; 13:458–465.
61. Swoap SJ, Overton JM, Garber G. Effect of ambient temperature on cardiovascular parameters in rats and mice: a comparative approach. *Am J Physiol Regul Integr Comp Physiol* 2004; 287:R391–R396.
62. Maloney SK, Fuller A, Mitchell D, Gordon C, Overton JM. Translating animal model research: does it matter that our rodents are cold? *Physiology (Bethesda)* 2014; 29:413–420.